ceramics

MDPI

Article

Effects of Translucency-Enhancing Coloring Liquids on the Mechanical Properties of 3Y- and 4Y-TZP Zirconia Ceramics

Andreas Pfeffer, Sebastian Hahnel, Angelika Rauch and Martin Rosentritt *

Department of Prosthetic Dentistry, UKR University Hospital Regensburg, 93042 Regensburg, Germany
* Correspondence: martin.rosentritt@ukr.de

Abstract

The aim of translucency-enhancing liquids (TEL) is to locally influence the phase composition of zirconia in order to increase its translucency. This study aimed to determine the influence of TEL on 3Y- and 4Y-TZP zirconia concerning roughness, hardness, wear, flexural strength, dynamic stability and fracture force of fixed dental prostheses after thermal cycling and mechanical loading. Two zirconia materials (4Y-TZP; 3Y-TZP-LA, n = 8 per material and test) were investigated with and without prior application of TEL. Two-body wear tests were performed in a pneumatic pin-on-block design (50 N, 120,000 cycles, 1.6 Hz) with steatite balls (r = 1.5 mm) as antagonists. Mean and maximum vertical loss as well as roughness (Ra, Rz) were measured with a 3D laser-scanning microscope (KJ 3D, Keyence, J). Antagonist wear was determined as percent area of the projected antagonist area. Martens hardness (HM; ISO 14577-1) and biaxial flexural strength (BFS; ISO 6872) were investigated. The flexural fatigue limit BFSdyn was determined under cyclic loading in a staircase approach with a piston-on-three-ball-test. Thermal cycling and mechanical loading (TCML: 2 × 3000 × 5 °C/55 °C, 2 min/cycle, H_2O dist., 1.2 × 10^6 force á 50 N) was performed on four-unit fixed dental prostheses (FDPs) (n = 8 per group) and the fracture force after TCML was determined. Statistics: ANOVA, Bonferroni test, Kaplan–Meier survival, Pearson correlation; $\alpha = 0.05$. TEL application significantly influences roughness, hardness, biaxial flexural strength, dynamic performance, as well as fracture force after TCML in 3Y-TZP. For 4Y-TZP, a distinct influence of TEL was only identified for BFS. The application of TEL on 3Y- or 4Y-TZP did not affect wear. TEL application has a strong effect on the mechanical properties of 3Y-TZP and minor effects on 4Y-TZP. All effects of the TEL application are of a magnitude that is unlikely to restrict clinical application.

Keywords: zirconia; translucency-enhancing liquid; surface roughness; hardness; biaxial strength; wear; dynamic loading; thermal cycling and mechanical loading; fracture force; dental materials

Academic Editors: Gilbert Fantozzi and Vincent Garnier

Received: 23 June 2025
Revised: 21 July 2025
Accepted: 21 July 2025
Published: 22 July 2025

Citation: Pfeffer, A.; Hahnel, S.; Rauch, A.; Rosentritt, M. Effects of Translucency-Enhancing Coloring Liquids on the Mechanical Properties of 3Y- and 4Y-TZP Zirconia Ceramics. *Ceramics* **2025**, *8*, 92. https://doi.org/10.3390/ceramics8030092

1. Introduction

Monolithic zirconia is used for the fabrication of fixed dental prostheses (FDPs) due to its excellent mechanical properties and tooth-colored appearance. Nevertheless, the low translucency of a specific zirconia might limit the tooth shade appearance of a restoration [1]. By doping the zirconia with yttria, the resulting grain size and thus the translucency of the zirconia can be influenced [2]. Therefore, zirconia is divided into different groups: 3Y-TZP is stabilized with 3 mol% yttria and is commonly the least translucent and strongest zirconia available. A higher proportion of yttria, such as in 4Y- and 5Y-TZP, increases the grain size and light transmission, but generally reduces strength. Multilayer zirconia are

combining high strength and good translucency by combining different types of zirconia in a single milling blank.

Translucency is observed when a light beam, which passes through a material is partially scattered, reflected and transmitted by the object [3]. As the amount of light that passes through the object increases, translucency also increases [4]. Light scattering is influenced by various elements such as voids and porosities, differing refractive indices or a high crystalline content [5]. Additional factors include the crystal number and size, particularly when the crystal particles are slightly larger than the wavelength of the incoming light [6].

An increased yttria content suppresses the phase transformation from tetragonal to monoclinic, which can be seen as the reason for the differences in translucency and mechanical properties [7]. The lower toughness and strength of materials with a higher yttria content (e.g., 4Y-TZP) compared to materials with a lower yttria content (e.g., 3Y-TZP) is directly attributable to inherent differences between the tetragonal and cubic zirconia phases. The changes in translucency are due to refractive index mismatches at the interfaces between the tetragonal and cubic phases, which lead to light scattering and reduce light transmission. This can be remedied by minimizing the volume fraction of the second phase or its structure size [3,8]. Doping ions from TEL stabilize the cubic zirconia phase and therefore have a significant effect on the densification behavior and final grain size. Possible mechanisms also include changes in defect concentrations and changes in grain boundary/interface properties [3].

Translucency-enhancing liquids (TELs) might represent an alternative or supplement to combine favorable general stability with locally enhanced translucency. As the liquid is applied to the incisal part of a restoration in order to increase the translucency in a very localized manner, the basal and cervical areas as well as the inner layer of the restoration are not affected, which are thus supposed to feature full stability. In order to influence the grain structure, the TEL is applied before final sintering. The liquid is supposed to infiltrate the porous material and locally increase the yttria content to up to 10 percent by weight. During sintering, this process leads to a coarsening of the grains and stabilizes the cubic structure, which ultimately increases light transmission [9]. A typical TEL consists of yttrium(III)–nitrate hexahydrate or yttrium carbonate hydrate, which is dissolved in hydrochloric or nitric acid [10]. Alternatives include magnesium, calcium or cerium compositions [3] or different solvents [11]. The solutions are usually used as dopant or precursor in the preparation of Yttrium-based materials [12]. The general effect of TEL on zirconia was shown by a study that revealed reduced fracture toughness and opacity in TEL-modified zirconia [13], but there are no studies considering the effects of TEL on the mechanical properties of zirconia. Therefore, this study focused exclusively on mechanical properties after TEL application. Since TELs are applied superficially and diffuse into the framework, it can be expected that the induced modifications can be characterized especially by superficial properties such as hardness [14,15], roughness [16] or wear stability [17,18]. It is possible that the changes induced by TEL-modification are so small that neither strength [14,19] nor the dynamic properties of the zirconia [20] are relevantly affected. Ultimately, only an examination of restorations under clinically relevant simulation conditions [21] may adequately assess the influence of the TEL on the stability of restorations. Fracture tests performed in restorations can help to detect damages such as cracks that occur during simulation and to specify differences between restorations with and without TEL. Against this background, the question arises as to what extent the mechanical properties of 3Y- and 4Y-TZP zirconia are affected by the application of TEL.

The null hypothesis of this investigation was that the application of TEL significantly reduces roughness, hardness, wear/antagonistic wear, flexural strength and dynamic

performance as well as the in vitro performance and fracture force after simulated aging in 3Y- and 4Y-TZP zirconias.

2. Materials and Methods

Two zirconia materials (DD cube one ML (4Y-TZP); DD Bio ZX2 color (3Y-TZP-LA)) were investigated with and without application of TEL (Incisal X; all Dental Direkt, Spenge, D). According to the safety data sheet, Incisal X contains 45-55 weight-% ytterbiumtrinitrat pentahydrate, and <0.5 weight-% hydrogen chloride. Test specimens and three-unit FDPs were dry milled (MCXL, Dentsply-Sirona, Charlotte, NC, USA) from each material and treated with TEL. Specimens were completely infiltrated and FDPs were either completely infiltrated or infiltrated only in cusp region.

The application was performed with a microbrush and specimens were dried for 20 min at 90 °C (TSU-S, Mihm-Vogt, Stutensee, D). For sintering, the standard sintering protocol was used: specimens were heated up to 900 °C at a rate of 8 °C/min, and a dwell time of 30 min, then heated up to 1450 °C at a rate of 3 °C/min with a dwell time of 120 min. Cooling was performed at a rate of 10 °C/min down to 200 °C (inFire HTC speed, Dentsply-Sirona, Charlotte, NC, USA).

All specimens were also investigated without prior infiltration with TEL for reference (Figure 1).

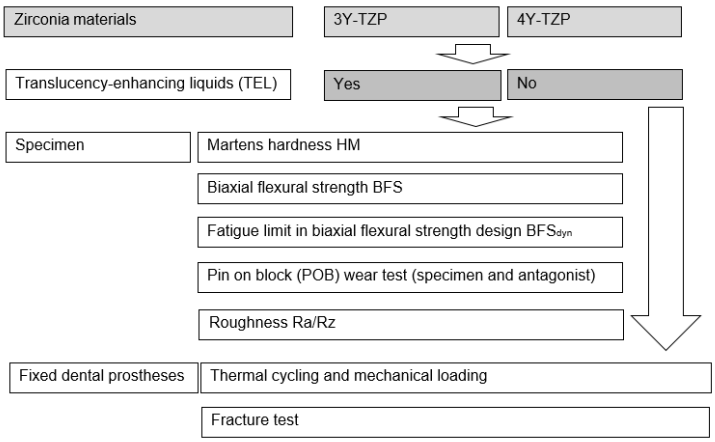

Figure 1. Study design.

Martens hardness (HM): Specimens were investigated using instrumented indentation testing (ISO 14577-1 [22]) in a universal hardness-testing machine (ZwickiLine Z2.5, ZwickRoell, Ulm, D). The indentation depth was constantly monitored at a loading speed of 0.1 mm/min to a maximum force of Fmax = 100 N using a Vickers indenter and a dwell time of 2 s. Unloading was performed at 0.1 mm/min. The recorded force-indentation depth curves were used to calculate HM. Poisson's ratio of the diamond indenter was set to $\nu i = 0.07$. Young's modulus of the indenter was Ei = 1140 GPa.

Biaxial flexural strength BFS: Biaxial flexural strength (BFS) was determined with a piston-on-three-ball test (ISO 6872 [23], Z010, ZwickRoell, Ulm, D). Specimens (ø = 16 mm, h = 2 mm) were positioned on a supporting ring-like bearing (THS1620, Grip-Engineering Thümler GmbH, Rastede, D) that consisted of three stainless steel spheres (Ø 3 mm), which were arranged in the form of an equilateral triangle at 120° (diameter = 10 mm). Specimens were placed centrally with a 0.05 mm thick polyethylene film (1-7090, neoLab Migge GmbH, Heidelberg, D) between the specimen and the piston as well as between the specimen and the bearing in order to evenly distribute contact forces. Specimens were preloaded with 0.5 N. The piston (diameter 1.6 mm) applied the load at 1 mm/min. The fracture force was measured and the biaxial flexural strength was calculated.

Fatigue limit in biaxial flexural strength design BFSdyn: The flexural fatigue limit was determined under cyclic loading in a staircase approach with a piston-on-three-ball test (ISO 6872). Specimens (ø = 16 mm, h = 2 mm) were positioned on a supporting ring-like bearing, consisting of three stainless steel spheres (Ø 3 mm), which were arranged in the form of an equilateral triangle at 120° (diameter = 10 mm). Specimens were centrally loaded with a piston (diameter 1.6 mm). In the stepwise loading test, each specimen was loaded with a dynamic force (Dynamess TP 5 HF, Stolberg, D; f = 10 Hz, 30,000 load changes per force step) in 250 N steps starting at 1000 N. The measured fracture force was used to calculate the biaxial flexural strength during dynamic loading BFSdyn. Number of cycles until failure was determined.

Pin on block (POB) wear test: Two-body wear tests were performed on eight specimens per group (8 × 2 mm, thickness: 2 mm) in a pneumatic pin-on-block design (Wear Tester, Inso, Lonnerstadt, Germany, vertical load 50 N, 120,000 cycles, 2.5 Hz; lateral movement = 1 mm, occlusal movement = 1 mm) with steatite balls (radius = 1.5 mm; magnesium silicate, CeramTec, Plochingen, D) as antagonists in a water bath. Mean and maximum vertical loss as well as roughness within (Ra, Rz) and besides the wear trace (Ra Ref, Rz Ref) were measured with a 3D laser-scanning microscope (KJ 3D, Keyence, J). Antagonist wear was determined as percent area of the projected antagonist area (Digital microscope, Keyence, Ōsaka, J).

Thermal cycling and mechanical loading (TCML): Artificial teeth with a preparation design suitable for all-ceramic restorations (tooth 16 and 14; preparation: thickness of 1.5 mm, n = 16 per group) were printed (Form 3B, Formlabs, Berlin, D). The roots of the teeth were coated with a layer of polyether impression material (1 mm thickness; Impregum, 3 M, St. Paul, USA) to simulate the resilience of the human periodontium. The teeth were fixed in resin bases (Palapress, Kulzer, Hanau, D) in a distance of 10 mm towards each other to simulate a three-unit FDP situation. FDPs were fabricated (n = 8 per group). The teeth and the intaglio surfaces of the FPDs were sandblasted (Al_2O_3, 1 bar, 50 µm), steamed, cleaned for 3 min in an ultrasonic bath (99% isopropanol) and dried. The inner surfaces of the FDPs were pretreated with a bonding agent for 60 s (UniBond, Dental Direkt, Spenge, D). The agent was applied with a disposable brush, left to act for 60 s and then carefully dried with oil-free air. The FPDs were adhesively bonded (Solid Link, Dental Direkt, Spenge, D) to the artificial teeth. Solid link was applied into the FPDs and the FPDs was inserted and held in position with slight pressure for 4 min. A small excess was removed after light curing. Final light polymerization was performed from four sides with a light curing unit for a period of 40 s for each side (1200 mW/cm^2; 385–515 nm; Bluephase G4, Ivoclar Vivadent, Schaan, FL).

TCML (2 × 3000 × 5 °C/55 °C, 2 min/cycle, temperature change during cycling within 30s; H_2O dist., 1.2 × 10^6 force á 50 N) was performed to simulate five years of clinical service. For all FDPs that survived TCML, the fracture force was determined (Z010, ZwickRoell, Ulm, D). The force was applied on the center of the FDPs by using a steel ball (diameter = 12 mm, v = 1 mm/min). A tin foil of 1 mm thickness was inserted between the crown and the steel ball to produce equal force distribution. The failure determination was set to a 10% loss of the maximum loading force or an acoustic signal (crack).

Statistics: Means and standard deviation were calculated (SPSS 29, IBM, Armonk, NY, USA). Comparisons between groups were performed using one-way ANOVA, Bonferroni post hoc test and Pearson correlation. Cumulated fatigue limit was calculated with Kaplan Maier Log Rank (Mantel-Cox) test. The level of significance was set to $\alpha = 0.05$.

3. Results

Martens hardness: Mean HM results for 3Y-TZP ranged between 9335.3 ± 356.9 MPa and 6458.1 ± 1604.9 MPa after infiltration with significant ($p < 0.001$) differences between infiltrated and non-infiltrated specimens. HM for 4Y-TZP showed values between 6444.8 ± 1271.4 N and 7090.4 ± 2152.7 N after infiltration without significant ($p = 0.477$) differences (Table 1).

Table 1. Mean and standard deviation (hardness: HM; biaxial flexural strength: BFS, dyn. Biaxial flexural strength, cycles until failure; *p*-values Anova, Bonferroni).

	Hardness HM [MPa]		Biaxial Flexural Strength BFS (MPa)		Dyn Biaxial Flexural Strength (MPa)		Cycles Until Failure (n)	
	Mean	**Std**	**Mean**	**Std**	**Mean**	**Std**	**Mean**	**Std**
3Y-TZP-LA	9335.3	356.9	1305.3	183.1	928.1	254.2	96,919	57,391
3Y-TZP-LA + full X	6458.1	1604.9	757.6	76.6	559.3	105.0	19,320	29,438
p=	<0.001		<0.001		0.008		0.015	
4Y-TZP	6444.8	1271.4	1157.7	178.0	967.9	70.2	111,525	24,208
4Y-TZP + full X	7090.4	2152.7	790.9	124.1	753.6	253.1	58,907	54,741
p=	0.477		<0.001		0.074		0.057	
ANOVA *p*=	0.002		<0.001		0.005		0.007	

Biaxial flexural strength: Mean BFS results for 3Y-TZP ranged between 1305.3 ± 183.1 MPa and 757.6 ± 76.6 MPa after infiltration with significant ($p < 0.001$) differences between the values. BFS for 4Y-TZP showed values between 1157.7 ± 178.0 N and 790.9 ± 124.1 N after infiltration with significant ($p < 0.001$) differences (Table 1).

Biaxial flexural strength dyn: Mean BFSdyn results for 3Y-TZP ranged between 928.1 ± 254.2 MPa and 559.3 ± 105.0 MPa after infiltration with significant ($p = 0.008$) differences between the values. BFSdyn for 4Y-TZP produced values between 967.9 ± 70.2 N and 753.6 ± 253.1 N after infiltration without significant ($p = 0.074$) differences. After infiltration, the number cycles until failure was significantly reduced for 3Y-TZP ($p = 0.015$) but not for 4Y-TZP ($p = 0.057$; Table 1). Log Rank (Mantel Cox) revealed significant differences in survival between reference and infiltrated groups of 3Y-TZP ($p = 0.020$) but not for those of 4Y-TZP ($p = 0.383$, Figure 2).

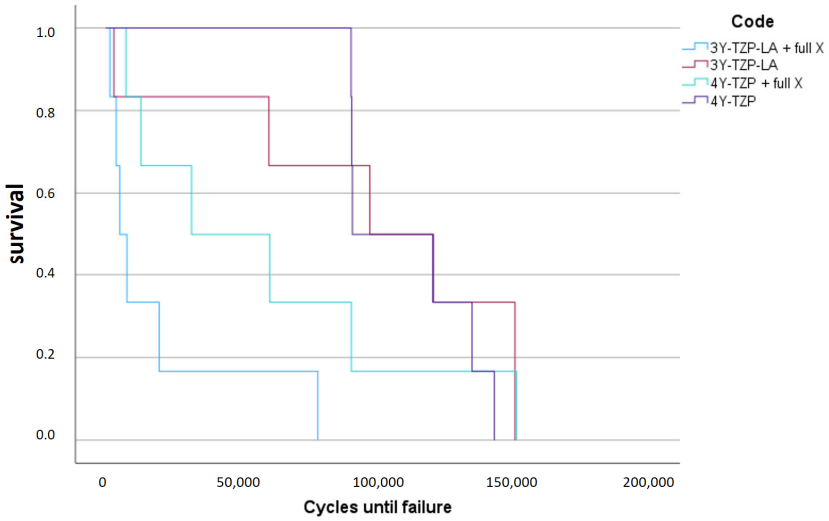

Figure 2. Survival curve (Log Rank Mantel Cox: different survival between reference and infiltrated groups of 3Y-TZP ($p = 0.020$) but not for the 4Y-TZP ($p = 0.383$)).

Wear: Mean wear results for 3Y-TZP ranged between −12.5 ± 5.8 µm and −15.5 ± 4.3 µm after infiltration. Wear for 4Y-TZP showed values between −11.5 ± 4.3 µm and 13.7 ± 6.2 µm

after infiltration. No significant differences were identified between the results ($p \geq 0.225$, Table 2).

Table 2. Mean and standard deviation (wear, maximum wear, wear antagonist; *p*-values Anova, Bonferroni).

	Wear [µm]		Wear Max [µm]		Wear Antagonist [%]	
	Mean	**Std**	**Mean**	**Std**	**Mean**	**Std**
3Y-TZP-LA	−12.5	5.8	−34.4	10.0	24.1	5.8
3Y-TZP-LA + full X	−15.5	4.3	−45.8	13.1	28.5	11.7
p=	0.255		0.070		0.351	
4Y-TZP	−11.5	3.1	−36.3	8.7	25.2	6.4
4Y-TZP + full X	−13.7	6.2	−39.8	10.5	24.8	6.4
p=	0.375		0.478		0.899	
ANOVA *p*=	0.421		0.131		0.689	

Wear max: Maximum wear for 3Y-TZP ranged between −34.4 ± 10.0 µm and −45.8 ± 13.1 µm after infiltration. Maximum wear for 4Y-TZP showed values between −36.3 ± 8.7 µm and 39.8 ± 10.5 µm after infiltration. No significant differences were identified.

Wear antagonist: Wear of the antagonist for 3Y-TZP ranged between -24.1 ± 5.0% and −28.5 ± 11.7% after infiltration. Wear of the antagonist for 4Y-TZP showed values between −25.2 ± 6.4% and 24.8 ± 6.4% after infiltration. No significant differences were identified between the results ($p \geq 0.351$, Table 2).

Roughness: Ra Ref values after fabrication ranged between 1.0 ± 0.3 µm (4Y-TZP) and 1.4 ± 0.8 (3Y-TZP-LA + full X) without significant ($p \geq 0.211$) differences between the groups. Ra results in the wear trace for 3Y-TZP ranged between 1.2 ± 0.4 µm and 1.8 ± 0.5 µm after infiltration with significant ($p = 0.011$) differences between the values. Ra results for 4Y-TZP ranged between 1.3 ± 0.4 µm and 1.7 ± 0.9 µm after infiltration without significant ($p = 0.131$) differences between the results (Table 3). Rz Ref values after fabrication varied between 8.3 ± 1.7 µm (4Y-TZP- + full X) and 13.1 ± 0.8 (3Y-TZP-LA + full X) without significant ($p \geq 0.075$) differences between the groups. Rz results for 3Y-TZP ranged between 10.6 ± 3.9 µm and 16.1 ± 4.8 µm after infiltration with significant ($p = 0.026$) differences between the values. Ra results for 4Y-TZP ranged between 12.0 ± 3.9 µm and 13.3 ± 5.9 µm after infiltration without significant ($p = 0.084$) differences between the results (Table 3).

Table 3. Mean and standard deviation (Roughness Ra, Rz in the wear trace and Ra, Rz reference; *p*-values Anova, Bonferroni).

	Ra [µm]		Ra Ref [µm]		Rz [µm]		Rz Ref [µm]	
	Mean	**Std**	**Mean**	**Std**	**Mean**	**Std**	**Mean**	**Std**
3Y-TZP-LA	1.2	0.4	1.0	0.5	10.6	3.9	8.7	1.2
3Y-TZP-LA + full X	1.8	0.5	1.4	0.8	16.1	4.8	13.9	1.8
p=	0.011		0.211		0.026		0.093	
4Y-TZP	1.3	0.4	1.0	0.4	12.0	3.9	8.4	1.3
4Y-TZP + full X	1.7	0.9	1.0	0.3	13.3	5.9	8.3	1.7
p=	0.229		0.888		0.603		0.940	
ANOVA *p*=	0.131		0.264		0.084		0.075	

Fracture force after TCML: Fracture forces after TCML for 3Y-TZP ranged between 1059.1 ± 243.4 N (3Y-TZP-LA), 1368.4 ± 289.0 N (3Y-TZP-LA + full X) and 1630.3 ± 476.9 N (3Y-TZP-LA + X). ANOVA comparisons revealed significant ($p = 0.036$) differences between the groups. Bonferroni comparisons showed significant ($p = 0.011$) differences in fracture force only between 3Y-TZP-LA and 3Y-TZP-LA + X. Fracture forces after TCML for 4Y-

TZP ranged between 1020.1 ±310.6 N (4Y-TZP), 1065.5 ± 337.2N (4Y-TZP + full X) and 881.3± 385.4 N (4Y-TZP + X). ANOVA (p = 0.784) and Bonferroni comparisons (p = 0.896) revealed no significant differences between the groups (Table 4).

Table 4. Mean and standard deviation (fracture force; p-values Anova, Bonferroni) and fracture pattern.

	Fracture Force [N]		**Fracture Pattern (n=)**		
	Mean	**Std**	**Co**	**CoMa**	**Cr**
3Y-TZP-LA	1059.1	243.4	2	6	
3Y-TZP-LA + full X	1368.4	289.0	1	2	5
3Y-TZP-LA + X	1630.3	476.9		4	4
p=	0.036				
4Y-TZP	1020.1	310.6	1	6	1
4Y-TZP + full X	1065.5	337.2	4	3	1
4Y-TZP + X	881.3	385.4	3	5	
p=	0.784				
ANOVA p=	0.001				

Fracture pattern was characterized as a fracture of the connector (Co) (n = 11) or at the crown (Cr) (n = 11). The highest number of failures was observed at the connector/margin (CoMa) (n = 24). With increasing infiltration, the number of failures at the crown increased for 3Y-TZP and the number of failures at the connector increased for 4Y-TZP.

For 3Y-TZP, significant correlations with infiltration could be identified for fracture force (0.578/p = 0.003), HM (0.798/p < 0.001), BFS (0.899/$p \leq$ 0.001), BFS dyn (0.720/p = 0.008), cycles until failure (0.682/p = 0.015), Ra (0.615/p = 0.011) and Rz (0.554/p = 0.026). For 4Y-TZP, a correlation between infiltration and BFS (0.783/$p \leq$ 0.001) could be determined.

4. Discussion

The hypothesis of this investigation suggesting that the application of TEL does significantly reduce roughness, hardness, wear/antagonistic wear, flexural strength and dynamic performance as well as the in vitro performance and fracture force after aging has to be partially rejected. In general, a distinct influence of TEL application was identified for most of the investigated properties in 3Y-TZP, whereas in 4Y-TZP only BFS was affected.

Martens hardness: Mean HM was about 30% lower for 3Y-TZP after infiltration, whereas 4Y-TZP showed no significant HM change after infiltration. Zirconia hardness is determined by the packing density and the strength of the atomic bonds [19]. The HM for infiltrated 3Y-TZP was at the same level as for 4Y-TZP, which suggests a similar structure. The reason for this phenomenon could be a change in phase configuration from a tetragonal to a cubic phase due to infiltration. However, whether the cubic phase is harder than the tetragonal phase depends on composition, fabrication conditions or porosity [24]. 3Y-TZP consists of about 100% tetragonal phase (tetragonal zirconia polycrystal (TZP)), whereas zirconia with a yttria content between 3 and 8 mol% has a tetragonal and cubic phase (partially stabilized zirconia (PSZ)) [7]. The fact that HM for 4Y-TZP hardly changed after infiltration could be a further indication that a corresponding phase was already existent. However, studies showed hardly a significantly different hardness for zirconia with different configurations [14], with HM between ~6500 and 7500 MPa. It must be clarified whether a possible reason for the change in the hardness of 3Y-TZP could also be the influence of TEL on aluminum oxide, which is added at the grain boundaries to increase the flexural strength and improve the durability. The manual application of the TEL proved to be very limited in its handling, which is why the resulting infiltration and reproducibility are not easy to control. This is certainly also reflected in the increase in standard deviations in HM after infiltration. The different deviations in the variability of

the HM in the two non-infiltrated groups may be due to a different homogeneity and pores in the material. Influences from surface roughness cannot be ruled out either.

Biaxial flexural strength: Zirconia's biaxial flexural strength typically falls within the range between 900 and 1200 MPa [25]. 3Y-TZP showed a significantly higher BFS in comparison to 4Y-TZP. The values observed in the current study confirm the principal differences but are considerably 20% higher than those reported in the literature [14]. This phenomenon certainly reflected the different composition, fabrication and treatment of the different commercially available zirconia materials [26,27]. Nevertheless, infiltration lowered mean BFS for both types of zirconia by around 30–40%. The weakening effect of TEL seemed to be higher for 3Y-TZP than for 4Y-TZP, resulting in an almost identical BFS for 3Y-TZP and 4Y-TZP after infiltration. The fact that the BFS after infiltration was at a similar level indicates a similar phase configuration of the zirconias in the tensile zone. Nevertheless, as in clinical routine TEL is only applied incisal or occlusal (pressure zone), the effects might be rated as uncritical.

Biaxial flexural strength dyn: 3Y-TZP showed no differences in BFSdyn in comparison to 4Y-TZP, which confirms earlier studies [19] providing almost identical values of ~500 MPa 3Y-TZP and of 550–600 MPa for 4Y-TZP. BFSdyn for 3Y-TZP decreased by 40% after infiltration, whereas BFSdyn for 4Y-TZP showed a loss of only 20%. This observation also suggests that the materials undergo different phase transformations. However, this assumption must be verified by EDX analysis or Raman spectroscopy. The influence of TEL on 3Y-TZP was much more evident, presumably due to a change from tetragonal and cubic phases. Starting from a comparable survival number, a stronger decrease for 3Y-TZP during testing indicated that 3Y-TZP is also more affected by TEL than 4Y-TZP. Only the infiltrated 3Y-TZP group showed failures that occurred much earlier during the dynamic tests, again indicating a significant modification due to infiltration. Zirconia polycrystals with higher tetragonal-phase content and lower cubic-phase content were supposed to feature better fatigue behavior [28]. Accelerated fatigue in general can help to analyze the lifetime of zirconia so that the specimens are exposed to loads greater than those occurring during mastication.

Wear: For both 3Y- and 4Y-TZP, mean and maximum wear showed only a slight increase after the application of TEL. The results without infiltration are comparable to previous data [17], where 3Y-TZP-LA-, 4Y-TZP- and 5Y-TZP showed comparable wear behavior with mean wear between 10 and 20 µm. Considering the generally low wear of the different zirconia types, these small differences would probably not be noticed in a clinical setting. In addition, antagonistic wear was not different between the different types of zirconia and after TEL infiltration. This could be due the fact that the coefficient of friction of zirconia is lower than that of other ceramics [29].

Roughness: For both materials, the reference roughness was comparable or even higher after TEL infiltration. Although the effects are measurable, they might be too small for producing a clinical effect. On the other hand, the increase in Ra and Rz for 3Y-TZP in the wear trace was more pronounced, again indicating a change in the phase of 3Y-TZP. Infiltrated material is roughened more pronouncedly than non-infiltrated zirconia. However, the altered surface roughness could have an effect on the wear of the FPDs and the antagonists. Particularly in the contact areas, this phenomenon could indicate higher or antagonistic wear in the long term. In addition, the altered roughness could have a negative effect on the color and gloss and thus the aesthetics of the restoration. While these results correspond to previous data [16], conflicting data [17] have also been published.

Fracture force after TCML: All FDPs survived TCML without failure, indicating the general usability of TEL in FDPs. Fracture forces of the non-infiltrated FDPs after TCML are in the range of comparable previous studies using non-infiltrated zirconia [21,30]. Contrary

to expectations, the application of TEL on 3Y-TZP even led to an increase of fracture forces after TCML. Local application, on the other hand, caused an even greater increase compared to complete infiltration of the FDP. The reason for this observation might be the local initiation of stress due to local phase transition. The localized occlusal application could build up compressive stress on the connectors and basal areas, which could lead to an increased strength of the FDPs. The application of TEL, in turn, appears to have an effect on the phase configuration and changes the stability of the restoration. However, an effect of different sintering behavior cannot be excluded [31].

In comparison, the application of TEL on 4Y-TZP did not result in obvious changes of fracture forces, but only a slight reduction due to partial application. Thus, small changes in fracture forces might be a confirmation of a limited effect of TEL on the phase and structure of 4Y-TZP. These observations match the results from the other tests in the current study, showing that 4Y-TZP is only partially affected by infiltration.

Fracture Pattern: Without TEL application, 3Y-TZP and 4Y-TZP showed no differences in fracture patterns, but the influence of TEL is obvious: with increasing infiltration, fractures of the crown became more frequent for 3Y-TZP. The effect of TEL on the connector in FDPs seemed apparently circumstantial compared to the effect on the crown. Infiltrating 4Y-TZP seemed to have a stronger impact on the connector than on the crown: without infiltration, the fracture line reached the crown margin in 75% of the cases, whereas fully infiltrated FDPs provided fracture mostly in the connector. This phenomenon could be an indicator of a reduction in flexural strength due to phase variation. A previous study [32] reported a fracture rate of 100% at the distal connector for 4Y-PSZ and 87.5% for 3Y-TZP. Nevertheless, distinct studies are difficult to compare because of the influence of the design of the restoration (influence connector cross-section; crown dimension) [33].

Fully covering an FDP with TEL is not recommended according to the instruction manual. However, the current study did not reveal problems resulting from an intentionally wrong application technique, as the fracture force for fully infiltrated 3Y-TZP was even higher than for standard 3Y-TZP. Different infiltration procedures did not affect 4Y-TZP. This phenomenon is important, because TEL might be accidentally applied on a connector. Nevertheless, local infiltration might cause unexpected effects as observed by the increase of force in 3Y-TZP after occlusal application. Manual application has been reported to be limited in handling and reproducibility and the resulting exact infiltration does not appear to be clearly controllable [9]. This is certainly also reflected in the high standard deviations after application. Overall, each test group in the current study still exceeded the maximum bite forces of approximately 500 N [34], which indicates that all groups can withstand clinical conditions.

The results show that the application of TEL caused changes in the zirconia and influenced its mechanical properties to varying degrees. Nevertheless, the effect of TEL on translucency and microstructure of the fused zirconia should be further investigated. A structural analysis seems mandatory to clarify the changes in the mechanical properties [35]. In addition, long-term studies must show how far the application of TEL can influence zirconia in the long-term. For example, it has been reported that the translucency of zirconia may increase with thermomechanical ageing [14].

5. Conclusions

The application of TELs significantly influences the properties of 3Y-TZP. The effect of TEL application was only minor on 4Y-TZP. TEL infiltration

- Resulted in a reduction of HM by approximately 1/3 for 3Y-TZP, while there was no effect for 4Y-TZP.
- Led to a 30–40% reduction in BFS for both types of zirconia.

- Resulted in a 40% reduction in BFSdyn for 3Y-TZP and a 20% reduction for 4Y-TZP.
- Had only a small effect on the wear behavior of the two zirconia types.
- Showed only minor effects and in some cases a slight increase in the roughness.
- Of 3Y-TZP, FPDs led to an increase in fracture forces, while for 4Y-TZP FPDs, it caused no obvious changes.
- Caused an increase in fractures in the crown region of the FPDs.

Author Contributions: Conceptualization, A.P. and M.R.; methodology, A.P.; software, A.P.; validation, A.P. and M.R.; formal analysis, A.P.; investigation, A.P.; resources, M.R.; data curation, A.P. and M.R.; writing—original draft preparation, A.P. and M.R.; writing—review and editing, A.P., M.R., S.H. and A.R.; visualization, A.P. and M.R.; supervision, M.R.; project administration, M.R.; funding acquisition, M.R. All authors have read and agreed to the published version of the manuscript.

Funding: This research received no external funding.

Institutional Review Board Statement: Not applicable.

Informed Consent Statement: Not applicable.

Data Availability Statement: The data presented in this article are available on request from the corresponding author. The data are not publicly available due to privacy.

Acknowledgments: We thank Dental Direkt, Spenge, D for providing materials.

Conflicts of Interest: The authors declare no conflicts of interest. The Dental Direkt, Spenge, D provided materials. The manufacture had no role in design of the study; in the collection, analyses or interpretation of data; in the writing of the manuscript; or in the decision to publish the results.

Abbreviations

The following abbreviations are used in this manuscript:

TEL	Translucency-enhancing liquid
FDP	Fixed dental prostheses
TZP	Tetragonal zirconia polycrystal
PSZ	Partially stabilized zirconia
HM	Martens hardness
BFS	Biaxial–flexural strength
BFSdyn	Fatigue limit in biaxial–flexural strength
POB	Pin on block wear test
TCML	Thermal cycling and mechanical loading
Co	Fracture at the connector
CoMa	Fracture at the connector/crown margin
Cr	Fracture of the crown

References

1. Lümkemann, N.; Pfefferle, R.; Jerman, E.; Sener, B.; Stawarczyk, B. Translucency, flexural strength, fracture toughness, fracture load of 3-unit FDPs, Martens hardness parameter and grain size of 3Y-TZP materials. *Dent. Mater.* **2020**, *36*, 838–845. [CrossRef]
2. Stawarczyk, B.; Keul, C.; Eichberger, M.; Figge, D.; Edelhoff, D.; Lümkemann, N. Three generations of zirconia: From veneered to monolithic. Part I. *Quintessence Int.* **2017**, *48*, 369–380. [CrossRef] [PubMed]
3. Dash, A.; Kim, B.-N.; Klimke, J.; Vleugels, J. Transparent tetragonal-cubic zirconia composite ceramics densified by spark plasma sintering and hot isostatic pressing. *J. Eur. Ceram. Soc.* **2019**, *39*, 1428–1435. [CrossRef]
4. Baldissara, P.; Llukacej, A.; Ciocca, L.; Valandro, F.L.; Scotti, R. Translucency of zirconia copings made with different CAD/CAM systems. *J. Prosthet. Dent.* **2010**, *104*, 6–12. [CrossRef] [PubMed]
5. Heffernan, M.J.; Aquilino, S.A.; Diaz-Arnold, A.M.; Haselton, D.R.; Stanford, C.M.; Vargas, M.A. Relative translucency of six all-ceramic systems. Part II: Core and veneer materials. *J. Prosthet. Dent.* **2002**, *88*, 10–15. [CrossRef]
6. Heffernan, M.J.; Aquilino, S.A.; Diaz-Arnold, A.M.; Haselton, D.R.; Stanford, C.M.; Vargas, M.A. Relative translucency of six all-ceramic systems. Part I: Core materials. *J. Prosthet. Dent.* **2002**, *88*, 4–9. [CrossRef]

7. Kongkiatkamon, S.; Rokaya, D.; Kengtanyakich, S.; Peampring, C. Current classification of zirconia in dentistry: An updated review. *PeerJ* **2023**, *11*, e15669. [CrossRef]
8. Xu, P.; Wang, H.; Cui, W.; Chen, Q.; Tu, B.; Sang, X.; Wang, W.; Fu, Z. $ZnO{\cdot}2.7Al_2O_3$ nanocomposite with high optical transparency. *J Am Ceram Soc.* **2022**, *105*, 3735–3739. [CrossRef]
9. Greitens, U.; Heilemann, N. Entfärbeliquid. German Patent No. 102015216056, 12 August 2016.
10. Hauptmann, H.; Herrmann, A.; Jahns, M.; Kolb, B. Translucency Enhancing Solution for Zirconia Ceramics. U.S. Patent No. 029743, 8 March 2013.
11. Wang, H.; Yan, Q.; He, L.; Zheng, Y. Method of Changing Translucent Properties of Zirconia Dental Materials. U.S. Patent No. 8697716B2, 26 June 2014.
12. Xia, C. Preparation of yttria stabilized zirconia membranes on porous substrates by a dip-coating process. *Solid State Ion.* **2000**, *133*, 287–294. [CrossRef]
13. Ban, S.; Yasuoka, Y.; Sugiyama, T.; Matsuura, Y. Translucent and Highly Toughened Zirconia Suitable for Dental Restorations. *Prosthesis* **2023**, *5*, 60–72. [CrossRef]
14. Jerman, E.; Lümkemann, N.; Eichberger, M.; Zoller, C.; Nothelfer, S.; Kienle, A.; Stawarczyk, B. Evaluation of translucency, Marten's hardness, biaxial flexural strength and fracture toughness of 3Y-TZP, 4Y-TZP and 5Y-TZP materials. *Dent. Mater.* **2021**, *37*, 212–222. [CrossRef]
15. Rohr, N.; Schönenberger, A.J.; Fischer, J. Influence of Surface Treatment and Accelerated Ageing on Biaxial Flexural Strength and Hardness of Zirconia. *Materials* **2023**, *16*, 910. [CrossRef] [PubMed]
16. Mitov, G.; Heintze, S.D.; Walz, S.; Woll, K.; Muecklich, F.; Pospiech, P. Wear behavior of dental Y-TZP ceramic against natural enamel after different finishing procedures. *Dent. Mater.* **2012**, *28*, 909–918. [CrossRef] [PubMed]
17. Rosentritt, M.; Preis, V.; Behr, M.; Strasser, T. Fatigue and wear behaviour of zirconia materials. *J. Mech. Behav. Biomed. Mater.* **2020**, *110*, 103970. [CrossRef] [PubMed]
18. Jitwirachot, K.; Rungsiyakull, P.; Holloway, J.A.; Jia-Mahasap, W. Wear Behavior of Different Generations of Zirconia: Present Literature. *Int. J. Dent.* **2022**, *2022*, 9341616. [CrossRef]
19. Arcila, L.V.C.; Ramos, N.d.C.; Campos, T.M.B.; Dapieve, K.S.; Valandro, L.F.; de Melo, R.M.; Bottino, M.A. Mechanical behavior and microstructural characterization of different zirconia polycrystals in different thicknesses. *J. Adv. Prosthodont.* **2021**, *13*, 385–395. [CrossRef]
20. Wendler, M.; Belli, R.; Valladares, D.; Petschelt, A.; Lohbauer, U. Chairside CAD/CAM materials. Part 3: Cyclic fatigue parameters and lifetime predictions. *Dent. Mater.* **2018**, *34*, 910–921. [CrossRef]
21. Strasser, T.; Schmid, A.; Huber, C.; Rosentritt, M. 4-Unit Molar Fixed Partial Dentures Made from Highly Translucent and Multilayer Zirconia Materials: An In Vitro Investigation. *Ceramics* **2022**, *5*, 99–107. [CrossRef]
22. *ISO 14577-1*; Metallic materials—Instrumented Indentation Test for Hardness and Materials Parameters. Part 1: Test Method. International Organisation for Standardisation: Geneva, Switzerland, 2015.
23. *ISO 6872*; Dentistry—Ceramic Materials. International Organisation for Standardisation: Geneva, Switzerland, 2024.
24. Gómez, S.; Suárez, G.; Rendtorff, N.; Aglietti, E. Relation between mechanical and textural properties of dense materials of tetragonal and cubic zirconia. *Sci. Sinter.* **2016**, *48*, 119–130. [CrossRef]
25. Durkan, R.; Deste Gökay, G.; Şimşek, H.; Yilmaz, B. Biaxial flexural strength and phase transformation characteristics of dental monolithic zirconia ceramics with different sintering durations: An in vitro study. *J. Prosthet. Dent.* **2022**, *128*, 498–504. [CrossRef]
26. Juntavee, N.; Juntavee, A.; Phattharasophachai, T. Biaxial Flexural Strength of Different Monolithic Zirconia upon Post-Sintering Processes. *Eur. J. Dent.* **2022**, *16*, 585–593. [CrossRef] [PubMed]
27. Öztürk, C.; Çelik, E.; Gönüldaş, F. Effect of different surface treatments on the biaxial flexural strength of zirconia ceramics. *J. Prosthet. Dent.* **2023**, *129*, 220.e1–220.e5. [CrossRef] [PubMed]
28. Kelly, J.R.; Cesar, P.F.; Scherrer, S.S.; Della Bona, A.; van Noort, R.; Tholey, M.; Vichi, A.; Lohbauer, U. ADM guidance-ceramics: Fatigue principles and testing. *Dent. Mater.* **2017**, *33*, 1192–1204. [CrossRef] [PubMed]
29. Dejak, B.D.; Langot, C.; Krasowski, M.; Klich, M. Evaluation of Hardness and Wear of Conventional and Transparent Zirconia Ceramics, Feldspathic Ceramic, Glaze, and Enamel. *Materials* **2024**, *17*, 3518. [CrossRef]
30. Rosentritt, M.; Preis, V.; Schmid, A.; Strasser, T. Multilayer zirconia: Influence of positioning within blank and sintering conditions on the in vitro performance of 3-unit fixed partial dentures. *J. Prosthet. Dent.* **2022**, *127*, 141–145. [CrossRef]
31. Attia, M.A.; Radwan, M.; Blunt, L.; Bills, P.; Tawfik, A.; Arafa, A.M. Effect of different sintering protocols on the fracture strength of 3-unit monolithic gradient zirconia fixed partial dentures: An in vitro study. *J. Prosthet. Dent.* **2023**, *130*, 908.e1–908.e8. [CrossRef]
32. Pöppel, M.L.; Rosentritt, M.; Sturm, R.; Beuer, F.; Hey, J.; Schmid, A.; Schmidt, F. Fracture Load and Fracture Patterns of Monolithic Three-Unit Anterior Fixed Dental Prostheses after In Vitro Artificial Aging-A Comparison between Color-Gradient and Strength-Gradient Multilayer Zirconia Materials with Varying Yttria Content. *J. Clin. Med.* **2022**, *11*, 4982. [CrossRef]
33. Yılmaz, O.; Göze Saygın, A.; Bolayır, G. Comparison of fracture resistance of implant-supported fixed prothesis substructure materials with different cross-sectional geometry. *BMC Oral Health* **2025**, *25*, 645. [CrossRef]

34. Linderholm, H.; Wennström, A. Isometric bite force and its relation to general muscle forge and body build. *Acta Odontol. Scand.* **1970**, *28*, 679–689. [CrossRef]
35. Zhang, Y. Making yttria-stabilized tetragonal zirconia translucent. *Dent. Mater.* **2014**, *30*, 1195–1203. [CrossRef]